GROWTH AND CHARACTERIZATION OF CRYSTALS OF THIOUREA SODIUM FLUORIDE

J.Jude Brillin[1] & P.Selvarajan[2] & U.Rajesh Kannan[3]
[1]Research Scholar, Reg.No. 7429, Physics Department, Manonmaniam Sundaranar University, Abishekapatti-627012, Tirunelveli, Tamilnadu, India.
[2]Associate Professor of Physics, Department of Physics, Aditanar College of Arts and Science, Tiruchendur-628216, Tamilnadu, India.
[3]Department of Physics, Kamaraj College, Tuticorin-628003, Tamilnadu, India.
(Affiliated to Manonmaniam Sundaranar University, Abishekapatti-627012, Tirunelveli, Tamilnadu, India)

Received: May 21, 2018 Accepted: June 30, 2018

ABSTRACT *Single crystals of thiourea sodium fluoride (TUSF) were grown successfully by aqueous solution growth with slow evaporation technique. The grown crystals were transparent and colourless. The critical nucleation parameters of the sample were determined at different super saturation values. The NLO property of the grown crystal was confirmed by Kurtz-Perry powder technique. The mechanical strength of the crystal was analyzed by Vickers microhardness test. LDT studies of TUSF crystal were carried out using a Nd: YAG laser and photoconductivity of the sample was measured using a photoconductivity set-up.*

Keywords: *Thiourea complex; single crystal; solution growth; NLO; SHG; microhardness; LDT; Photoconductivity*

1. Introduction

Semiorganic nonlinear optical crystals are obtained by combining organic and inorganic materials in particular molar ratios and these materials are the technologically important crystals due to their applications in the field of optoelectronics, frequency conversion, optical telecommunication, image processing, optical computing, and data storage. Advances have been accounted recently in the field of nonlinear optics in the area of materials engineering and the associated optoelectronic device technologies [1, 2]. Thiourea is an interesting nonlinear optical (NLO) crystal and its metal complexes are the semiorganic NLO materials. Several researchers have grown and studied variety of thiourea complex NLO crystals and reported in the literature [3-6]. A variety of thiourea complex crystals have attracted great interest because these metal–organic complexes combine the high optical nonlinearity and chemical flexibility of organic materials with the physical characteristics of inorganic materials [7-10]. The thiourea metal complexes have an impact on frequency conversion, laser technology, telecommunication, optical computing and data storage technology and it is well known that thiourea is capable of forming a number of coordination compounds with various metals [11, 12]. In this work, a semi organic NLO crystal viz., thiourea sodium fluoride (TUSF) was synthesized and grown in the form of single crystals. The grown crystals of TUSF were characterized by nucleation kinetic studies, XRD studies, SHG studies, mechanical studies and optical studies and the obtained results are discussed.

2. Synthesis and crystal growth of thiourea sodium fluoride

The salt of thioruea sodium fluoride was synthesized by mixing AR grade thioruea and sodium fluoride in the equimolar ratio in double distilled water as solvent. The reaction of synthesis is adhered by the chemical equation $NH_2CSNH_2 + NaF \rightarrow NH_2CSNH_2.NaF$. The purity of the synthesized salt was further improved by repeated re-crystallization. The aqueous saturated solution of the re-crystallized salt of thiourea sodium fluoride (TUSF) was prepared at room temperature (31 ^oC) and the solution was stirred well for about 3 hours using a hot plate magnetic stirrer to ensure homogeneous concentration over entire volume of the solution. The solution was filtered using the good quality Whatman filter paper and transferred to a crystal growth vessel and crystallization was allowed to take place in a constant temperature bath (accuracy $\pm$ 0.01 ^oC) by slow evaporation technique. Seed crystals of TUSF were obtained from spontaneous nucleation and some good quality seed crystals were placed in the growth vessel containing the supersaturated aqueous solution of TUSF. Since the solution is supersaturated, seed crystals will not be dissolved. The seed crystals were grown into big-sized crystals of TUSF. The harvested crystal of TUSF is shown in the figure 1. It is observed that the grown crystal is transparent and colourless and the dimensions of the crystal are observed to be 16 x 14 x 8 mm^3.

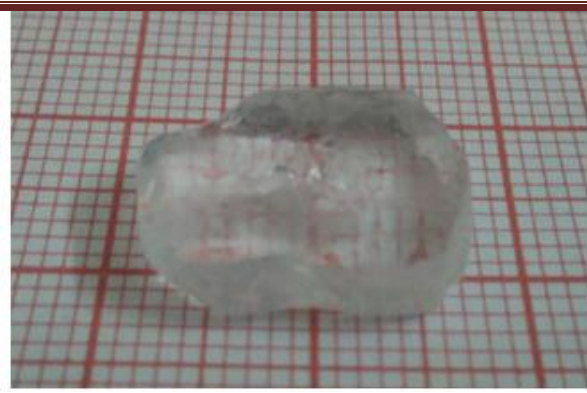

Fig. 1: A harvested single crystal of TUSF

3. Determination of critical nucleation parameters

Crystallization process has two main processes containing nucleation which is the birth of a nucleus and crystal growth which involves the subsequent growth of the existing nucleus. Nucleation is defined as the series of atomic or molecular processes by which the atoms or molecules of a reactant phase rearrange into a cluster of the product phase large enough to have the ability to grow irreversibly to a macroscopically larger size. Nucleation can be classified into two type namely primary nucleation and secondary nucleation. Primary nucleation is further classified into homogeneous and heterogeneous nucleations. Homogeneous nucleation takes place in the absence of foreign particles such as ions, impurity molecules and dust particles or surface of the container and Heterogeneous nucleation takes place in the presence of foreign particles in the supersaturated solution. Secondary nucleation takes place when nucleation is induced by the presence of crystals of the same substance. Irreversible nucleation takes place after the critical nuclei are formed in supersaturated solution. To analyze the critical nucleation process in the supersaturated solution, induction period was measured at various supersaturation ratios. The values of induction period were used to determine the critical nucleation parameters of TUSF sample [13, 14]. The induction period is defined as the time elapsed between the achievement of a supersaturated solution and the observation of first speck of TUSF crystal. Induction period of the TUSF salt was measured using isothermal and direct vision observation method. The ratio of the supersaturated concentration (C) to the saturated concentration (C_o) at the particular temperature is known as supersaturation ratio (S) and is given by $S = C/C_o$. Using this relation, the supersaturated concentration for the selected supersaturation ratio was found out. The values of induction period were measured for S = 1.2, 1.24, 1.28, 1.32, 1.36 and the plots of induction period and supersaturation ratio for TUSF are shown in the figure 2. It is observed that the induction period decreases as the supersaturation ratio increases. According to classical nucleation theory, the free energy barrier to nucleation is called the Gibbs free energy and the induction period ( ) in terms of Gibbs free energy is given by $\ln \tau = -B + \Delta G/kT$ where B is a constant, k is the Boltzmann's constant and T is the absolute temperature. The Gibbs free energy will be maximum for a certain value of radius (r*) of nucleus, which is known as critical radius. Once the critical nuclei are formed, they will not dissolve in the supersaturated solution again. The interfacial energy is the interface between the growing crystal and the surrounding mother phase which plays an important role in the nucleation of crystals. The complete theory of nucleation is given in the literature [15]. The important equations for calculating the critical nucleation parameters are: interfacial tension $(\sigma) = (RT/N)\,[3m/16\pi v^2]^{1/3}$ where R is the universal gas constant, v is the volume of a molecule (v = volume of unit cell / number of molecules per unit cell), m is the slope of the plot of ln τ versus $1/(\ln S)^2$ of TUSF crystal and N is the Avogadro's number, the size of the critical nucleus (r^*) and critical Gibbs free energy change (G) are given by $r^* = 2\sigma v N / RT \ln S$ and $\Delta G^* = mRT / [N (\ln S)^2]$ respectively and the number of molecules in a critical nucleus is found using equation $n = (4/3)$ (/v) r^3. The number of crystals produced in the supersaturated solution is expressed as nucleation rate i.e. the number of crystals produced per unit volume per unit time. The nucleation rate (J) can be calculated using the equation $J = A \exp [-\Delta G^*/(kT)]$ where A is the pre-exponential factor [16].

The slope of the plot of ln τ versus $1/(\ln S)^2$ for TUSF crystal was obtained from the figure 3 and the critical nucleation parameters such as Gibbs free energy change, interfacial tension, the radius of critical nucleus, the number of molecules in the critical nucleus and the nucleation rate were determined for TUSF crystal. The plots of Gibbs free energy change and nucleation rate for TUAF sample are shown in the figure 4 and the plots of radius of critical nucleus and number of molecules in the critical nucleus for TUSF sample are presented in the figure 5. It is seen that Gibbs free energy change, radius of critical nucleus and number

of molecules in the critical nucleus are decreasing with increase of supersaturation ratio and nucleation rate is observed to be increasing with increase of supersaturation ratio. The calculated value of interfacial tension for TUSF crystal is 1.472 x 10^{-3} J/m^2. The results show that when the supersaturation is increased, the number of crystal nuclei formed in the solution will be increased and this will lead to spurious nucleation. The low values of nucleation rate indicate the formation of multi-nuclei in the solution will be less in the less supersaturation level and hence large-sized crystals of TUSF could be grown when low supersaturation is used in the crystal growth conditions [17].

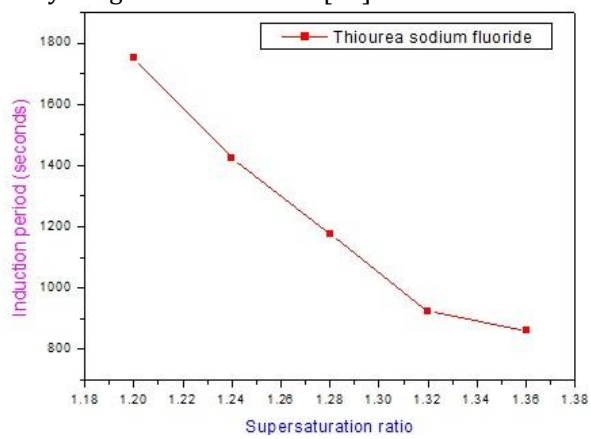

Fig.2: Plot of induction period versus supersaturation ratio for TUSF salt

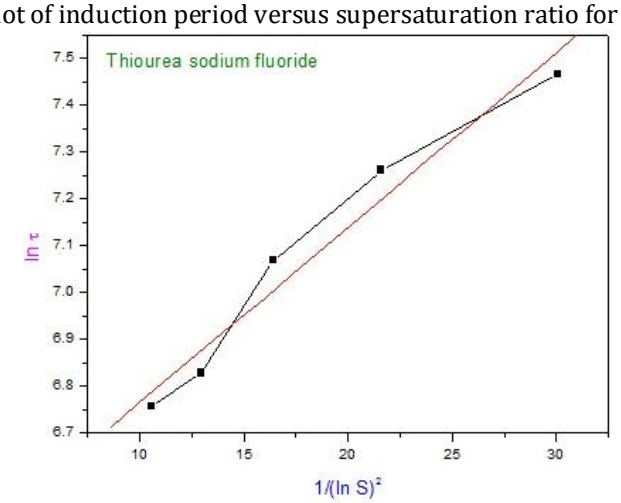

Fig.3: Plot of ln τ versus $1/(\ln S)^2$ of TUSF crystal

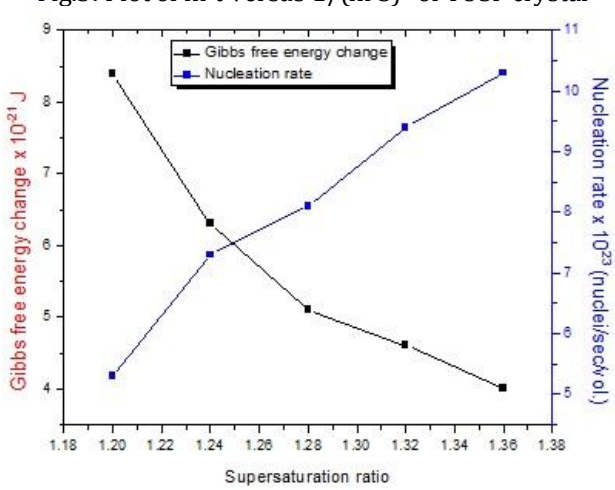

Fig.4: Variations of Gibbs free energy change and nucleation rate with supersaturation ratio for TUAF sample

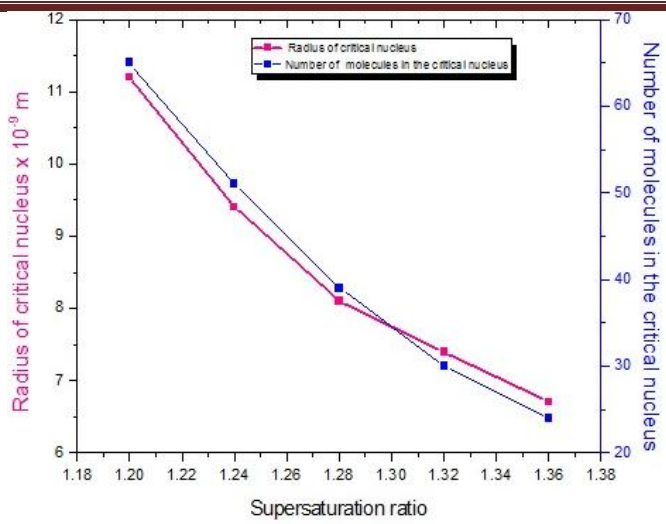

Fig.5: Plots of radius of critical nucleus and number of molecules in the critical nucleus with supersaturation ratio for TUSF sample

4. Microhardness, work hardening coefficient and resistance pressure

There are mechanical parameters such microhardness, stiffness constant, work hardening coefficient and yield strength and these parameters can be used to check the mechanical strength of materials. Microhardness test provides the useful information on the strength and deformation characteristics of the material. Using the values of microhardness of a crystal, the mechanical parameters can be evaluated. In the present study, microhardness measurement was performed using Vickers microhardness Leitz. Wetzlar tester. Here the indenter used was a diamond pyramidal indenter on the sample. After applying a suitable mini load on the indenter, an impression is formed on the specimen and the microhardness is calculated from the area or depth of indentation produced on the sample. In the static indentation test, the indenter is pressed perpendicularly in the surface of the sample by means of an applied load and by measuring the cross sectional area or the depth of the indentation and knowing the applied load, the microhardness number is calculated using the relation $H_v = 1.8544\ P/d^2$ where P is the applied load and d is the average diagonal indentation length of the impression on the sample and 1.8544 is a constant of the geometrical factor for the diamond pyramidal indenter. The calculated values of microhardness for different applied mini loads for TUSF crystal are presented in the figure 6. The results indicate that the hardness increases with increase of the applied load upto 75 g and then it decreases. The increasing part is due to reverse indentation size effect and the decreasing part is due to normal indentation size effect [18, 19].

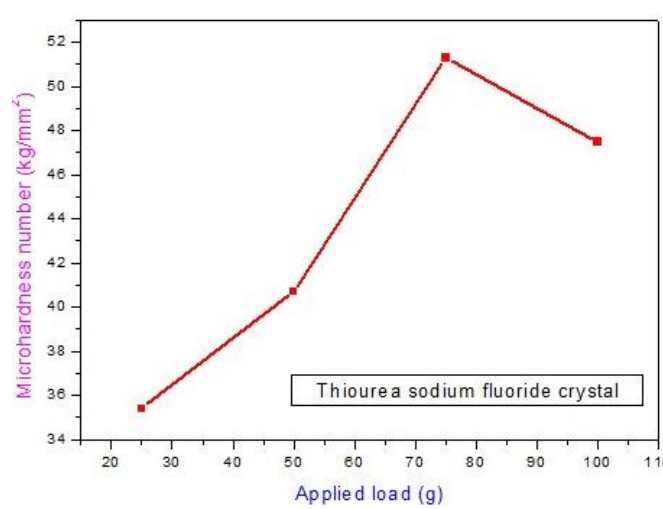

Fig.6: Variation of microhardness number with the applied load for TUSF crystal

Meyer established a relationship between indentation hardness and work hardening capacity of a material [20] and it is given by $P = a\ d^n$, where a is a constant and n is work hardening coefficient for a given material. The value of 'n' can be considered as a parameter representing the capacity for work hardening or Meyer

index and it is determined from log P = log a + n log d, the slope of the line plotted between log d and log P gives the value of work hardening coefficient and it was obtained to be 2.6152 from the plot of log P versus log d (Fig. 7). According to theory of hardness, $1.0 \leq n \leq 1.6$ for hard materials and $n > 1.6$ for soft materials and it is concluded that TUSF crystal belongs to the soft category of materials. Hays-Kendall's method can be used to find the resistance pressure of the material and according to Hays-Kendall's approach, the relation connecting load and the resistance pressure is $P = W + Ad^2$ where P is the applied load, d is the average diagonal indentation length, W is the minimum load to initiate plastic deformation in gram or resistance pressure, A is the load-independent constant [21] Using this relation, the plot between P versus d^2 is drawn and it is shown in the figure 8. The relation used to find the corrected indentation size independent hardness (H_o) is H_o=1.8544 A. The calculated value of resistance pressure (W) is -12.9554 g and the value of H_o for TUSF crystal is 0.0547 g/ μm². The resultant value of W becomes negative and hence the sample exhibits behaviour of reverse indentation size effect.

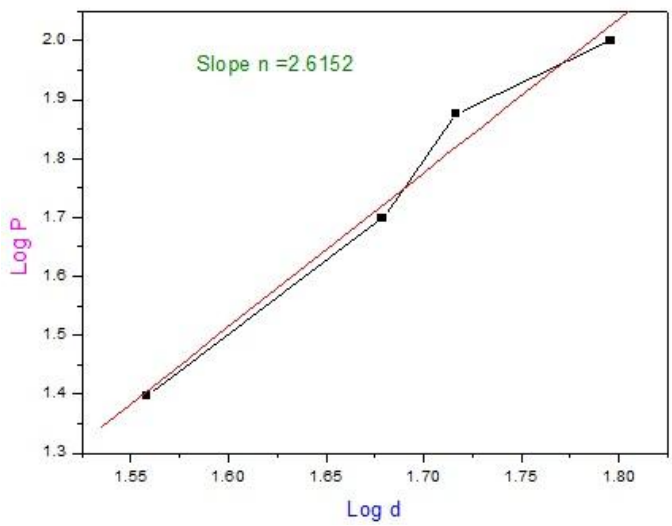

Fig.7: Plot of log P versus log d for TUSF crystal for obtaining work hardening coefficient

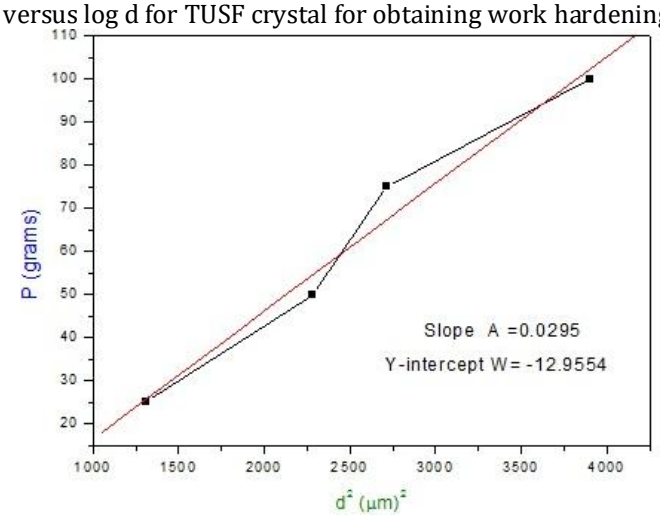

Fig.8: Plot of log P versus log d for TUSF crystal for obtaining the resistance pressure

5. Second order NLO studies

Nonlinear optics (NLO) is the study of interaction of intense electromagnetic field with materials to produce modified fields that are different from the input field in phase, frequency or amplitude. Second harmonic generation (SHG) is a nonlinear optical process that results in the conversion of an input optical wave into an output wave of twice the input frequency. The laser light propagated through a crystalline solid, which lacks a center of symmetry, generates light at second and higher harmonics of the applied frequency. The frequency doubling process is commonly called as second harmonic generation (SHG) and this study was carried out by Kurtz – Perry powder technique using a high intensity Nd: YAG laser (λ=1064 nm) with pulse duration of 8 ns. The SHG was confirmed by the emission of green radiation which was

detected by a photomultiplier tube. In this study Potassium Dihydrogen Phosphate (KDP) was used as the reference crystal. The SHG efficiency for TUSF crystal is found to be 1.07 times that of KDP sample.

6. Measurement of dark conductivity and photoconductivity

Photoconductivity is a phenomenon in which the conductivity of a material increases when light falls on it and this study was carried out using a photoconductivity set-up with a Keithley 485 picoammeter at room temperature (30 ^{o}C). Initially, in the absence of passing light on the sample, dark current was measured and then by passing light from halogen lamp (100 W) on the sample, photocurrent was measured. Both dark currents and photo currents of the electroded TUSF crystal were measured by applying various DC electric fields. The variations of dark and photo currents with different applied electric fields for TUSF crystal are presented in the figure 9. It is seen from the figure that the values of dark current and photo current increase with increase of applied electric field. For TUSF crystal, it is observed that the photo current is more than dark current and hence the sample has positive photoconductivity. The positive photoconductivity of the sample is due to increase of charge carriers when light is passed onto the sample [22].

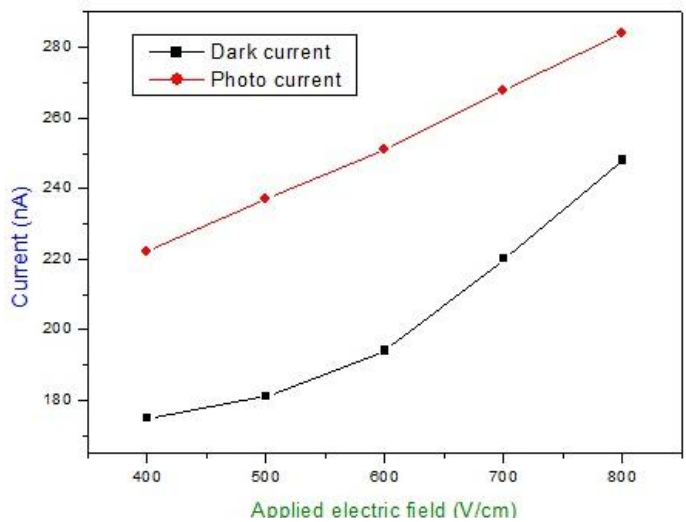

Fig.9: Plots of photo current or dark current versus electric field for TUSF crystal

7. Laser damage threshold studies

Laser damage threshold (LDT) study is an important for NLO crystals and using this study the laser damage limit of sample crystal is known. Laser damage threshold (LDT) study for TUSF crystal was carried out using a high intense Nd: YAG laser (1064 nm, 18 ns pulse width) and the laser energy was measured by Coherent energy/power meter. The value of LDT was calculated using the formula P= E/ $\tau\pi r^2$ where τ is the pulse width in ns, E is the input energy in mJ, r is radius of the spot in mm [23]. The calculated value of LDT of TUSF crystal is 0.492 GW/cm^2 and this value of found to be more than that of KDP crystal (0.2 GW/cm^2).

8. Conclusions

Slow evaporation technique was adopted to grow the single crystals of thiourea sodium fluoride. Critical nucleation parameters such as Gibbs free energy, nucleation rate, critical radius, interfacial tension and number of molecules in the critical nucleus of TUSF sample in the aqueous solution were determined by classical nucleation theory. The powder SHG measurement of the sample was carried out and the obtained value of SHG of TUSF crystal is 1.07 times that of KDP. The LDT value of TUSF crystal was obtained to be 0.492 GW/cm^2. From photoconductivity studies, it is confirmed that TUSF crystal has the positive photoconductivity. The mechanical properties like hardness, work hardening coefficient and resistance pressure of TUSF crystal were studied.

Aknowledgments

The author (J.Jude Brillin) is grateful to Manonmaniam Sundaranar University, Tirunelveli for permitting her to carry out the research work. The authors are thankful to the staff members of St Joseph College, Trichy, Cochin University, Crescent Engineering College, Vandaloore and VIT, Vellore for collecting the research data.

References

1. Xiue Ren, Dongli Xu, Dongfeng Xue, Crystal Growth 310 (2008) 2005-2009.
2. Dongfeng Xue, Henryk Ratajczak, Chem. Phys. Lett. 371 (2003) 601 – 607.
2. 3.P. A.Angelimary and S.Dhanuskodi,Cryst. Res. Technol. 11(2001) 1231–37.
3. V.Venkataraman, M.R.Srinivasan, H.L. Bhat, J. Raman Spectrosc. 25 (1994) 805–11.
4. S.Selvakumar, J.J. Packiam, Rajasekar S A, Ramanand A and Sagayaraj P, Mater. Chem. Phys. 93(2005) 356–60.
5. S.G.Bhat , S.M. Dharmaprakash, Mater. Res. Bull., 33 (1998) 833–40.
6. K. Ambujam, P.C. Thomas, S. Aruna, D. Prem Anand, P. Sagayaraj, Crystal Research and
7. Crystal Technology 41 (2006) 1082–1088.
8. S.G. Bhat, S.M. Dharmaprakah, Journal of Crystal Growth 181 (1997) 390–394.
9. V. Venkatramanan, S. Maheswaran, J.N. Sherwood, H.L. Bhat, Journal of Crystal Growth 179 , (1997) 605–610.
10. V. Kannan, N.P. Rajesh, R.B. Ganesh, P. Ramasamy, Journal of Crystal Growth 269 (2004) , 565–569.
11. Sweta Moitra, Tanusree Kar, Mater. Chem. Phys. 106 (2007) 8.
12. G. Bhagavannarayana, S.K. Kushwaha, S. Parthiban, G. Ajitha, S. Meenakshi Sundaram, J. Cryst. Growth 310 (2008) 2575.
13. S.Boomadevi, R.Dhanasekaran, P.Ramasamy, Cryst.Res.Technol. 37(2-3), (2002) 159-168
14. P.Santhanaraghavan, P. Ramasamy, Crystal Growth Processes and Methods, KRU Publication, Kumbakonam, Tamil Nadu, India (2003).
15. A.Siva Dhas, P.Selvarajan, T.H.Freeda, J.Mater. Manufact. Process. 24 (2009) 584-589.
16. M. Shah, O. Galkin, and P. G. Vekilov, J. Chem. Phys. 121 (2004) 7505.
17. R.Sankar, C.M.Ragavan and R.Jayavel , Cryst.Res.Technol.40(9) (2006) 919-924.
18. P.N.Kotru, A.K.Razdan, B.M.Wanklyn, J. Mater. Sci. 24 (1989) 793.
19. S.Mukerji, T.Kar, Cryst. Res. Technol. 34 (1999) 1323.
20. E.Meyer, Z. Phys. 9 (1908) 66.
21. C.Hays and E.G.Kendall, Metallography, 6, (1973) 275–282.
22. 22.G. Prabagaran, M. Victor Antony Raj, S. Arulmozhi and J. Madhavan, Der Pharma Chemica, 3 (6) (2011) 643-650.
23. M.Magesh, G.Ananda Babu, P.Ramasamy, J. Crystal Growth, 324 (2011)201-206.